Journal of Alloys and Compounds 509 (2011) 7861–7869

Contents lists available at ScienceDirect

Journal of Alloys and Compounds

journal homepage: www.elsevier.com/locate/jallcom

Theoretical investigation for Li_2CuSb as multifunctional materials: Electrode for high capacity rechargeable batteries and novel materials for second harmonic generation

Ali Hussain Reshak[a,b,*], H. Kamarudin[b]

[a] Institute of Physical Biology-South Bohemia University, Nove Hrady 37333, Czech Republic
[b] School of Materials Engineering, University Malaysia Perlis (UniMAP), P.O Box 77, d/a Pejabat Pos Besar, 01000 Kangar, Perlis, Malaysia

ARTICLE INFO

Article history:
Received 10 September 2010
Received in revised form 28 March 2011
Accepted 30 March 2011
Available online 6 April 2011

PACS:
70
71.15.Ap
71.1
71.15.−m

Keywords:
Rechargeable Batteries
Cu_2Sb
Li_2CuSb
Structural
Optical properties
DFT
GGA
FPLAPW

ABSTRACT

Based on the first-principles electronic structure calculations, we predict that Li_2CuSb should be good electrode materials for high capacity rechargeable batteries and novel materials for second harmonic generation. This prediction is based on the experimental measurements of Fransson et al. [1], and as step forward to do deep investigation on these materials we addressed ourselves for performing theoretical calculation. We found that intercalation of lithium leads to phase transitions, which agrees well with the experiment, increasing the conductivity of the material, and break the symmetry along the optical axis making the material useful for second harmonic generation (SHG) applications. We should emphasize that lithiated compound show very high second order optical susceptibility. We present the total charge densities in the (1 1 0) and (1 0 0) planes for the parent and lithiated phases and it was found that the parent compound shows a considerable anisotropy between the two planes in consistence with our calculated optical properties. We found that Li_2CuSb possesses high second harmonic generation and its second order optical susceptibility of the total absolute value at zero frequency is equal to 142 pm/V. Based on the value of the second order optical susceptibility the microscopic second order hyperpolarizability, β_{ijk}, the vector component along the dipole moment direction is about 31.01×10^{-30} esu.

1. Introduction

Never before has our daily life and environment been so significantly dependent on materials. Among the various categories of materials: novel materials for new long life rechargeable batteries, materials and the devices based on them play an important role which is increasing every year with the advent of modern technologies and their implementation in every day life. The quest for development of novel more efficient and compact rechargeable batteries requires a search for the design and fabrication of new materials which should be less expensive, more flexible, require less energy and more apt specific applications. Now-a-days these batteries are much required for different applications for example high durability medicine batteries, powering electric vehicles in order to improve the air quality in congested cities and as alternative energy future resources. The development of novel promising materials opens the possibilities for many new long lasting, high capacity batteries. The rechargeable lithium ion batteries is a device that fulfill the crucial demands of our modern society acting as the power source of various portable devices and in the future is expected to be used in electric vehicles and so on. Fransson et al. [1] studied structural evaluation in the Cu_2Sb anode using the in situ x-ray diffraction technique. They pointed out that lithium first reacted with Cu_2Sb to form the lithiated phase Li_2CuSb which was similar to its parent compound Cu_2Sb, and further lithium insertion into Li_2CuSb led to Li_3Sb. The data shows that Li is inserted into Cu_2Sb with a concomitant extrusion of Cu which initiates a phase transition to a lithited zinc-blende-type structure and further lithiation results in the displacement of the remaining Cu to yield Li_3Sb [1]. During these two steps reaction, Cu metal were extruded, and electrodes gained good electrical conductivity, showing good cycle performance. The large irreversible capacity at the first cycle precluded its commercial success as an anode in rechargeable ion batteries [2]. Thackeray

* Corresponding author at: Institute of Physical Biology-South Bohemia University, Nove Hrady 37333, Czech Republic. Tel.: +420 777 729583, fax: +420 386 361231.
E-mail address: maalidph@yahoo.co.uk (A.H. Reshak).

0925-8388/$ – see front matter © 2011 Elsevier B.V. All rights reserved.
doi:10.1016/j.jallcom.2011.03.179

et al. [3] presented an overview of several systems, particularly those that operate by lithium insertion/metal displacement reaction with a host metal array at room temperature, based on the attempts that those systems show strong structural relationships between a parent structure and its lithiated products. Ren et al. [4] attempted a novel process to prepare nanoscale Cu_2Sb and alloy powders as anode materials for lithium ion batteries. The nanoscale Cu_2Sb alloy showed good cyclability with a stable specific capacity of 200 mA/h g^{-1} within 25 cycles. Matsuno et al. [2] constructed ternary phase diagram for the Li–Cu–Sb system to elucidate the reaction mechanism upon charge–discharge reaction. We should emphasize that such ternary compounds May be also promising for the photoinduced nonlinear optical effects [5].

Mosby and Prieto [6] described the direct single potential electrodeposition of crystalline Cu_2Sb as promising anode material for lithium ion batteries, from aqueous solutions at room temperature using citric acid as a complexing agent. Sharma et al. [7] studied the mechanism of lithium insertion/intercalation in the anode materials InSb and Cu_2Sb using first principle total energy calculations. Morcrette et al. [8] have demonstrated that Cu_2Sb electrodes can operate reversibly in lithium cells. They describe the reactivity of lithium with Cu_2Sb to be governed by displacement reactions of Cu similar to those occurring in $Cu_{2.33}V_4O_{11}$. The search for novel materials with promising structural in order to use them as multifunctional materials for example; materials for researchable batteries and as nonlinear optical materials is still a challenge for scientists. The theoretical methods of studying the relationship between structure, electrochemical and the optical properties may be a better solution before venturing into the physical growth of the crystals. The *ab initio* calculations were extensively applied for the computations of some essential structural and some important properties for examples band structure, density of states, electron charge densities, electrochemical and optical properties. Further, the efficiency of these properties is inherently dependent upon its structural features. On the other hand, in recent years, density functional theory (DFT) has become an increasingly useful tool to examine experimental studies. The success of DFT is mainly due to the fact that it describes small molecules more reliably than Hartree–Fock theory. It is also computationally more economic than wave function based methods with inclusion of electron correlation [9,10]. Phase equilibria in alloys to great extent are governed by the ordering behavior of alloy species. One of the important goals of alloy theory is therefore to be able to simulate these kinds of phenomena on the basis of first principles for more details see the references [2,7,11,12].

As natural extension to our previous work on lithium batteries [13] we addressed ourselves to investigate electrode materials for high capacity rechargeable batteries. Among these electrode materials is Cu_2Sb intercalated with lithium to get the lithiated phase Li_2CuSb. Based on the experimental work of Fransson et al. [1], and Thackeray et al. [3] which is show there should be a strong structural relationship exists between the parent and the lithiated compounds, we performed a theoretical calculations for the band structure and density of states to find the relationship between the structure of the parent and the lithiated compound.

To the best of our knowledge no comprehensive work (experimental or theoretical) on the band structure, total and partial density of states, linear and nonlinear optical susceptibilities of Cu_2Sb and the nonlinear optical properties, band structure, total and partial density of states for Li_2CuSb compounds has appeared in the literature. We thought it would be interesting to begin a systematic theoretical study of the electronic properties of these compounds. We hope that our work will lead to more experimental and theoretical studies of these compounds which are interesting and useful multi-functional materials for rechargeable batteries and nonlinear optical properties. A detailed description of the electronic structure, the electrochemical and optical properties using a full potential method is very essential and would bring us important insights in understanding the origin of the electronic structure, the electrochemical and optical properties. We present calculations that are based on the full potential linear augmented plane wave (FP-LAPW) method which has proven to be one of the accurate methods [14,15] for the computation of the electronic structure of solids within a framework of density functional theory (DFT).

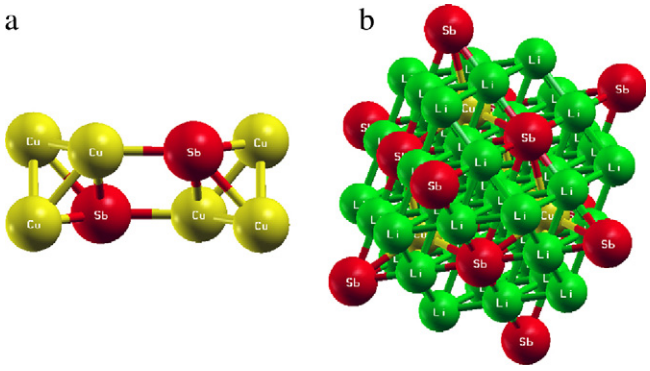

Fig. 1. Calculated crystal structure; (a) parent compound (b) intercalated compound.

This paper is organized as follows: Section 2, shows the method of calculations. In Section 3, we present our results of the calculations, and discuss the origin of band structure, charge density distribution, density of states, the electrochemical and spectral optical properties. Summary of our work is given in Section 4.

2. Method of calculation

In this paper, we perform the first-principles electronic structure calculations based on the generalized gradient approximation (GGA) [16] in the density functional theory (DFT) [17], using the full potential linearized augmented plane wave (FP-LAPW) method as incorporated in WIEN2K code [18]. In this method the space is divided into an interstitial region (IR) and non-overlapping muffin-tin (MT) spheres centered at the atomic sites. In the IR region, the basis set consists of plane waves. Inside the MT spheres, the basis sets is described by radial solutions of the one particle Schrödinger equation (at fixed energy) and their energy derivatives multiplied by spherical harmonics. The parent compound is crystallized in tetragonal structure space group ($P4/nmm$) with two formula units per unit cell. The unit cell parameters are $a = 3.97$ Å and $c = 6.06$ Å, the Cu atoms are situated at (0.75 0.25 0.0) and (0.25 0.25 0.27) and Sb atom at (0.25 0.25 0.7) positions. When we intercalated Cu_2Sb with Li, a phase transition occurs from tetragonal to cubic structure space group (F-43m) with unit cell parameters, $a = 6.28$ Å, in excellent agreement with experimental data [1,3]. The two Li atoms situated at (0.25 0.75 0.5) and (0.5 0.5 0.5), Sb at (0 0 0) and Cu at (0.75 0.75 0.75) positions. The crystal structures of the parent and the intercalated compounds are illustrated in Fig. 1.

In order to achieve energy eigenvalues convergence, the wave functions in the interstitial regions were expanded in plane waves with a cut-off $K_{max} = 9/R_{MT}$, where R_{MT} denotes the smallest atomic sphere radius and K_{max} gives the magnitude of the largest K vector in the plane wave expansion. The muffin-tin radii were assumed to be 2.0 atomic units (a.u.) for Cu and Sb of the parent and 1.39 a.u. for Li, 1.57 a.u. for Cu, and 2.09 a.u. for Sb of the lithiated phase Li_2CuSb. The valence wave functions inside the spheres are expanded up to $l_{max} = 10$ while the charge density was Fourier expanded up to $G_{max} = 14$ (a.u.)$^{-1}$. Self-consistency is obtained using 300 **k**-points in the irreducible Brillouin zone (IBZ). The BZ integration was carried out using the tetrahedron method [19,20]. The linear optical properties are calculated using 500 **k**-points and the nonlinear optical properties are calculated using 1400 **k**-points in IBZ. The self-consistent calculations are considered to be converged when the total energy of the system is stable within 10^{-5} Ry.

3. Results and discussion

3.1. Band Structure and density of states

To investigate the role the metal Cu plays in the band structure, and the effect of Li intercalation on it, we calculated the band structure, the total and partial density of states. Following the band structure and the densities of states (Figs. 2 and 3) one can conclude

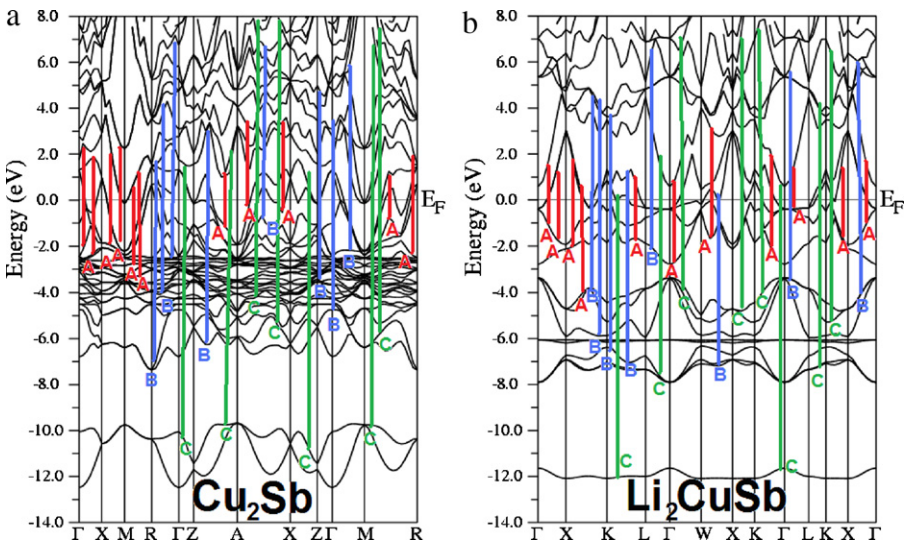

Fig. 2. Calculated band structure; (a) parent compound (b) intercalated compound.

that intercalation of lithium in the parent materials leads to phase transitions from tetragonal to cubic structure, and pushing the conduction and valence bands towards lower and higher energies with respect to Fermi energy (E_F), resulting in increasing the bandwidth as shown in Fig. 2b. The band structure and the total density of states (TDOS) along with the Cu-s/p/d, Sb-s/p/d, and Li-s/p partial density of states (PDOS) for Cu_2Sb and Li_2CuSb compounds are shown in Figs. 2 and 3. For the parent compound, the band structure and DOS can be divided into two group/structures. From the PDOS we are able to identify the angular momentum characters of various structures; the energy range from −13.0 to −9.0 eV is mainly originated from Sb-s and Cu-s/p. The energy region from −8.0 eV and above is originated from Cu-s/p/d and Sb-p/d. When we intercalated Li into Cu_2Sb, we noticed that Li leads to change the physical properties of the intercalated compound. The band structure and density of states of the intercalated compound can be divided into three group/structures; the lowest group/structure around −12.0 eV has mainly Sb-s with small contribution of Li-s/p and Cu-p. The second group/structure between −8.0 up to −3.0 eV is composed of Cu-d with a small contribution of Sb-p/d, Cu-s/p and Li-s/p. The third group/structure started from −3.0 eV and above has admixture of Cu-s/p, Sb-p/d and Li-s/p. From the PDOS of the parent compound we noticed a strong hybridization between Cu-p and Cu-s at around −10.0 eV, at around −3.0 eV, Cu-p hybridize with both Cu-s and Sb-d. Cu-p hybridizes with Cu-s at around 2.0 and 3.0 eV, at 2.0 eV Cu-s hybridize with Sp-s. Whereas for the intercalated compound Cu-s strongly hybridize with Sb-p at around −6.0 and 1.0 eV. In the energy ranges from −5.0 to −3.0 eV, 0.0 to 3.0 eV, and around −12.0 eV there exist strong hybridization between Li-p and Cu-p at around −8.0 eV, Li-s/p hybridize with Sb-d. We found that for the parent compound Cu-s/p and Sb-s/p/d states control the overlapping around Fermi energy (E_F) while Cu-s/p, Sb-p/d and Li-s/p are controlling the overlapping for the intercalated compound. The DOS at E_F is determined by the overlap between the valence and conduction bands. This overlap is strong enough, indicating a metallic origin with DOS at E_F, $N(E_F)$, of 25.84 states/Ry-cell for the parent compound and 32.64 states/Ry-cell for Li_2CuSb. The electronic specific heat coefficient (γ), which is function of DOS, can be calculated using the expression

$$\gamma = \frac{1}{3}\pi^2 N(E_F) k_B^2$$

Here, $N(E_F)$ is the density of states at E_F, and k_B is the Boltzman constant. The calculated energy density of states at the E_F enables us to calculate the bare electronic specific heat coefficient which is found 4.482 mJ/mol K^2 for the parent compound and 5.662 mJ/mol K^2 for Li_2CuSb compound. The Li-s and Li-p bands are very broad and contribute much to the density of states. Our calculations show a strong structural relationship exists between the parent and the lithiated compounds in excellent agreement with the experimental data [1,3] which shows that for good and high capacity rechargeable batteries it should be there is a strong structural relationship between the parent and the lithiated compounds [1,3].

Our calculations revealed that the electronic band structure and DOS are influenced significantly with the presence of lithium. The volume expansion for the transition from Cu_2Sb to Li_2CuSb is calculated to be 26.5% which is in very good agreement with the experimental data (26.5%) [21].

The origin of chemical bonding can be elucidated from the total and partial electronic densities of states. We find that the densities of states, extending from −8.0 eV up to Fermi energy (E_F) for the parent and intercalated compounds, is larger for Cu-d states (6.5 electrons/eV), Cu-s states (0.19 electrons/eV), Sb-p states (0.22 electrons/eV), Cu-p states (0.1 electrons/eV), for the parent compound. While for the intercalated compound Cu-d states (24.0 electrons/eV), Cu-s states (0.21 electrons/eV), Sb-p states (0.5 electrons/eV), Cu-p states (0.05 electrons/eV), Li-s states (0.06 electrons/eV), and Li-p states (0.19 electrons/eV). This is obtained by comparing the total densities of states with the angular momentum projected densities of states of Cu-s/p/d and Sb-p for the parent and Cu-s/p/d, Sb-p and Li-s/p states for lithiated phase as shown in Fig. 3. These results show that some electrons formed by Cu-s/p/d, Sb-p and Li-s/p terms are transferred into valence bands (VBs) and contribute in weak covalent interactions between Sb–Sb, Cu–Cu and Li–Li atoms, and the substantial covalent interactions between Sb and Cu, Cu and Li, Sb and Li atoms.

The effect of Li intercalation on the electron density was studied by plotting the electron densities before and after intercalation (Fig. 4a–d). The bonding nature of the solids can be described accurately by using electron charge density plots [22,23]. The charge density in our calculation is derived from a reliable converged wave function and hence it can be used to study the bonding nature of the solid. To visualise the nature of the bonding character and to explain the charge transfer and bonding properties we calcu-

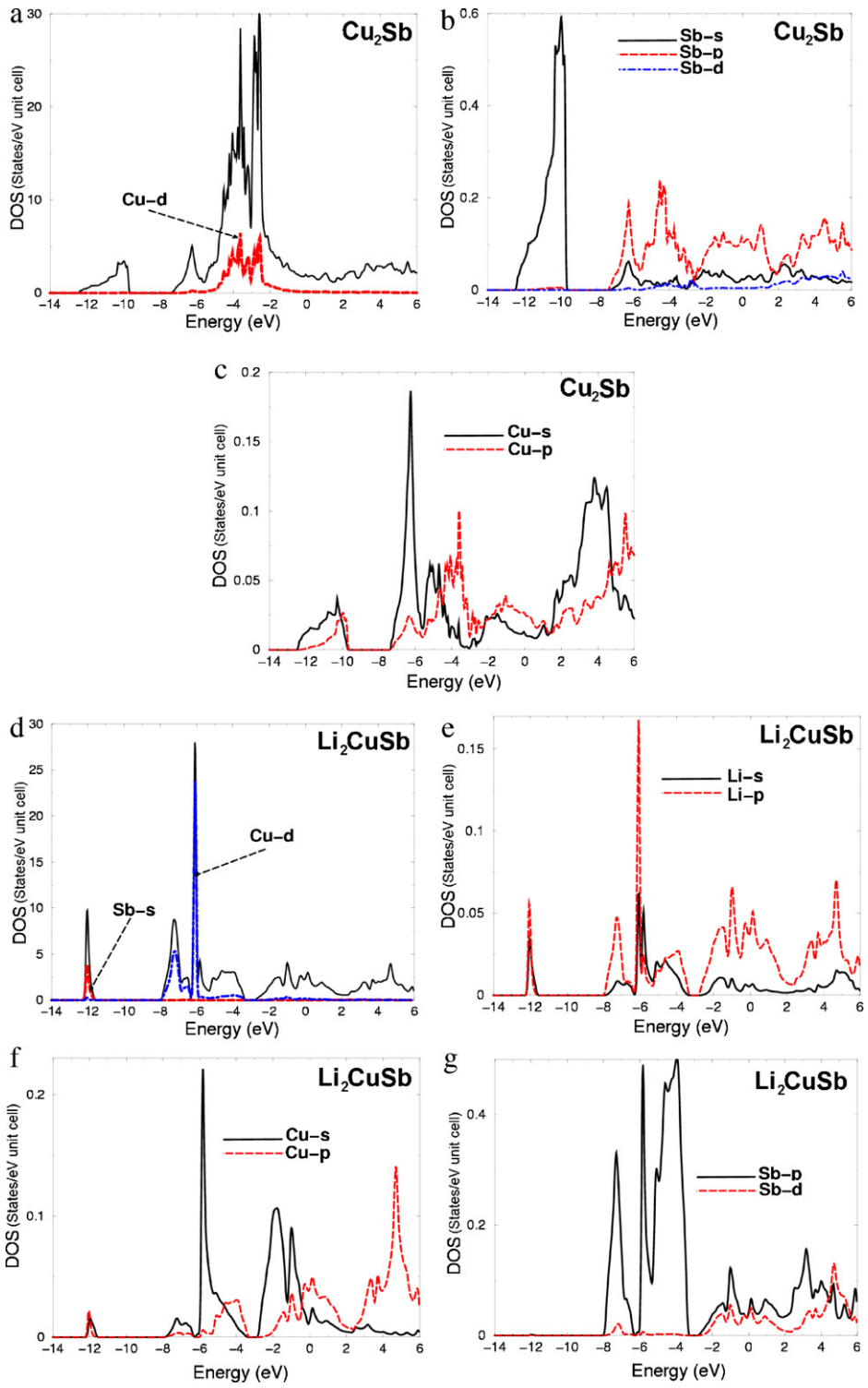

Fig. 3. Calculated total density of states (states/eV unit cell) along with the partial densities of states.

lated the total valence charge density. In Fig. 4 a–d, the total charge density distribution in the (1 1 0) and (1 0 0) planes for the parent and the lithiated phase Li_2CuSb were presented. Following these Figures we noticed that parent compound shows a considerable anisotropy between the two planes (see Fig. 4 a and b), whereas the lithiated phase show isotropic nature (see Fig. 4 c and d), that is another evidence of the phase transition occurs after the intercalation of lithium in the parent material. The charge densities help us to analyze the nature of the bonds in this compound according to a classical chemical concept. This concept is very useful to classify compounds into different categories with different chemical and physical properties. The valence electrons on intercalated lithium atoms are found to donate to the host material. For the bulk Cu2Sb which is a covalently bonded material and a strong covalent character for Cu–Sb bonding can be seen. One can see that the electronic charge density between Cu and Sb atoms decreases when Li atoms are intercalated in the Cu_2Sb. This indicates that the strength of Cu–Sb covalent bonding decreases when Li intercalation increases.

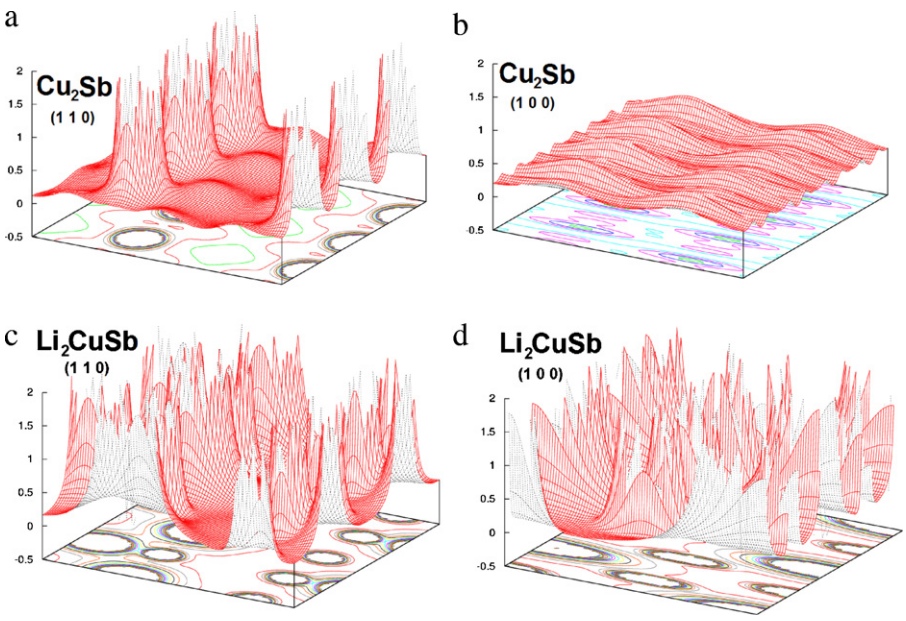

Fig. 4. Electron charge densities (a) parent compound for (1 1 0) plane (b) parent compound for (1 0 0) plane (c) parent compound for (1 1 0) plane (d) intercalated compound for (1 0 0) plane.

3.2. The electrochemical properties

The electrochemical properties of the parent and the lithiated compounds are measured and discussed extensively by Fransson et al. [1], and Thackeray et al. [3]. Due to the superior electrochemical characteristics found on Li_2CuSb we are interested in performing theoretical investigation focused on this compound as lithium batteries. We present here a first principles investigation on the electrochemical properties. First principles calculations have been widely used to predict the average voltage of lithium insertion in many compounds [24–35]. The interaction reaction of the lithium ion per formula unites is written as:

$$Cu_2Sb + 2Li^+ + 2e^- \rightarrow Li_2CuSb + Cu^{(0)} \quad (1)$$

in which $2e^-$ are involved in the electrochemical cell. The average lithium insertion voltage for this reaction can be obtained from the total energy differences using FP-LAPW without the need for the experimental data. Attempts to obtain intercalation voltages with first principles calculations are limited and have focused solely on the band structure of the materials:

$$V = \frac{E_{total}(Cu_2Sb) + 2E_{total}(Li^+) - E_{total}(Li_2CuSb) - E_{total}(Cu)}{zF} \quad (2)$$

where F is the Faraday constant, z is the charge (in electrons) transported by lithium in the electrode, E_{total} refers to the total energy per formula unite. With this methodology we predict a lithium insertion voltage of 2.78 V for the Li/Cu_2Sb, in good agreement with experimental value (3.0 V) [1]. The calculated average voltage of the insertion reaction is merely a measure of the relative stability of the inserted and deinserted materials. Besides predicting the insertion voltage, the first principles calculations also supply relevant information regarding other key factors affecting the electrochemical behavior of an electrode material. Among those factors, the reversibility of the insertion reaction (and finally the long term cycleability of the lithium battery) is closely related to the relationship between the crystalline structures of inserted and deinserted materials.

3.3. The role of structure in electrochemical reactions

The band structure of intercalation compounds has been studied extensively using FP-LAPW method. Since the host material is typically little affected structurally by the intercalation of lithium, and lithium is fully ionized to Li^+. It is believed that Li is fully ionized in most lithium-metal and donates its electron to the host bands without much affecting them. This makes it possible to control the band filling of the host material by varying the Li content electrochemically. The Structure plays an important role in the reversibility of electrochemical reactions, particularly those involving topochemical processes [36]. As we had mentioned before there should be a strong structural relationship exists between the parent and the lithiated compounds [1,3]. The reactions of lithium with metals and intermetallic compounds tend to be accompanied by a significant increase in crystallographic volume as it had found that it was 26.5%. Insertion of lithium in Cu_2Sb cause to complete displacement of one atom of Cu to yield a new binary phase:

$$Cu_2Sb + 2Li^+ + 2e^- \rightarrow Li_2CuSb + Cu^{(0)}$$

Lithium first reacts with Cu_2Sb to form the lithiated zinc-blende structure Li_2CuSb. During this reaction, the fcc Sb array which is slightly distorted in Cu_2Sb, provides a stable framework for lithium and copper. The transition for Cu_2Sb to Li_2CuSb involves the extrusion of 50% of copper atoms from the structure and a small internal displacement of the remaining Cu atoms to generate the CuSb zinc-blende framework. The Sb array expands by 25% during the transformation of Cu_2Sb to Li_2CuSb [1]. The reversibility and rate of this reaction is facilitated by the compatibility in the size and charge of the lithium and copper atoms and by absence of any significant internal displacement of Sb during the transformations. According to the experimental work [1]; apart from an irreversible capacity loss on the initial cycle, this electrode has shown excellent reversibility yielding 90% of its theoretical capacity. The good electrical conductivity of the extruded copper, the apparent absence of copper whiskers and exaggerated grain growth, and the strong structural relationship that exists between the parent and the lithiated compounds are considered to be the main reasons for the good electrochemical behavior of this electrode.

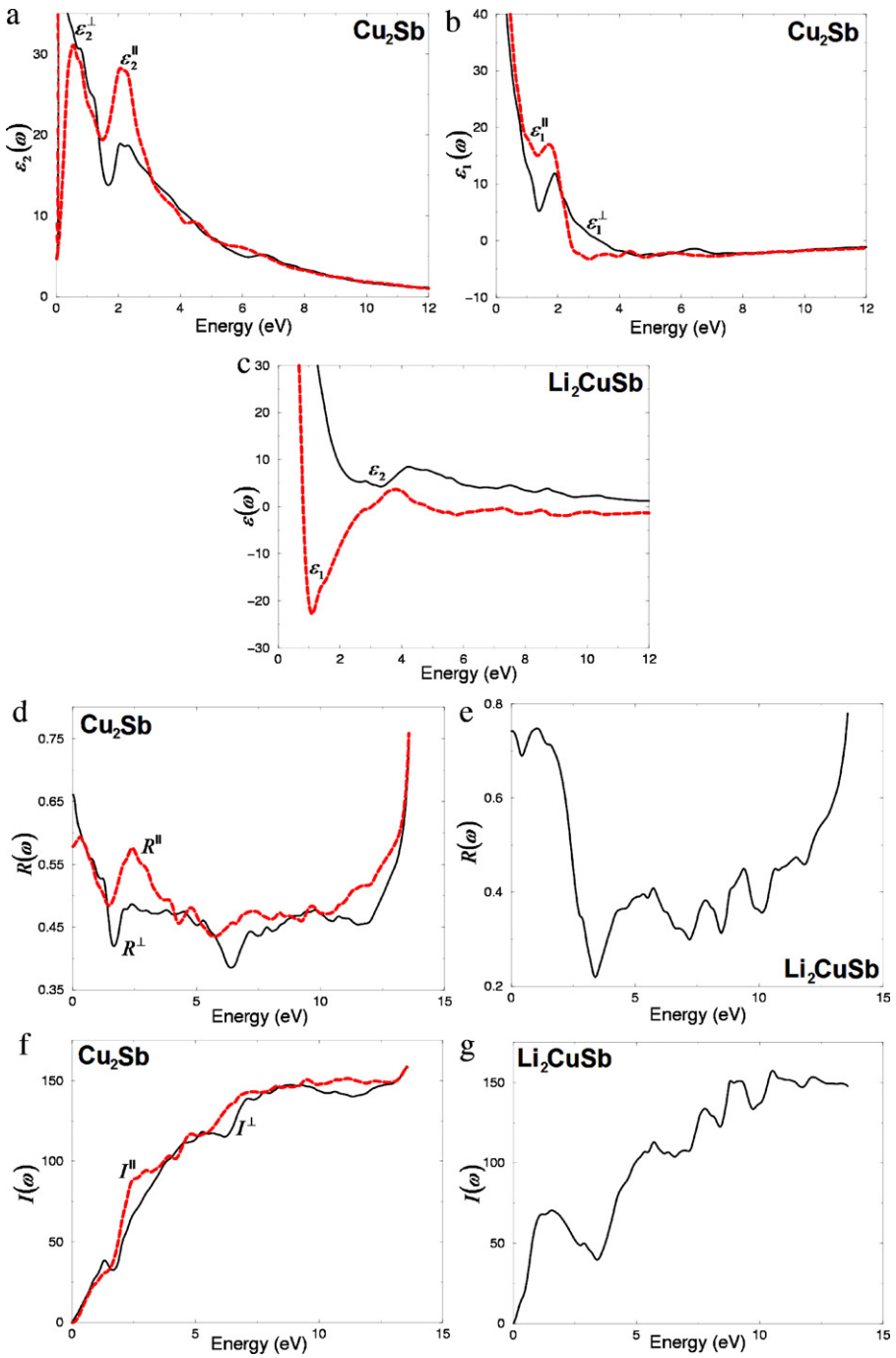

Fig. 5. (a) Calculated $\varepsilon_2^{\perp}(\omega)$ (dark solid curve) and $\varepsilon_2^{\mathrm{II}}(\omega)$ (light dashed curve) for parent compound. (b) Calculated $\varepsilon_2^{\perp}(\omega)$ (dark solid curve) and $\varepsilon_2^{\mathrm{II}}(\omega)$ (light dashed curve) for parent compound. (c) Calculated $\varepsilon_2(\omega)$ (dark solid curve) and $\varepsilon_1(\omega)$ (light dashed curve). (d). Calculated $R^{\perp}(\omega)$ (dark solid curve) and $R^{\mathrm{II}}(\omega)$ (light dashed curve) for parent compound (e) Calculated $R(\omega)$ for intercalated compound.

3.4. Linear optical properties

The optical properties of solids are a major topic, both in basic research as well as for industrial applications. While for the former the origin and nature of different excitation processes is of fundamental interest, the latter can make use of them in many optoelectronic devices. These wide interests require experiment and theory. Cu_2Sb crystallizes in the tetragonal structure space group $P4/nmm$. This symmetry group has two dominant components of the dielectric tensor. The experiments are performed with electric vector $\vec{E}$ parallel or perpendicular to the **c** axis. The corresponding dielectric functions are $\varepsilon^{\mathrm{II}}(\omega)$ and $\varepsilon^{\perp}(\omega)$. The calculations of these dielectric functions involve the energy eigenvalues and electron wave functions. These are natural outputs of band structure calculations. We have performed calculations of the imaginary part of the inter-band frequency dependent dielectric function using the expressions in the reference [37,38]

$$\varepsilon_2^{\mathrm{II}}(\omega) = \frac{12}{m\omega^2}\int_{BZ}\sum \frac{\left|P^{Z}_{nn'}(k)\right|^2 dS_k}{\nabla\omega_{nn'}(k)} \tag{3}$$

$$\varepsilon_2^{\perp}(\omega) = \frac{6}{m\omega^2}\int_{BZ}\sum \frac{\left[\left|P^{X}_{nn'}(k)\right|^2 + \left|P^{Y}_{nn'}(k)\right|^2\right] dS_k}{\nabla\omega_{nn'}(k)} \tag{4}$$

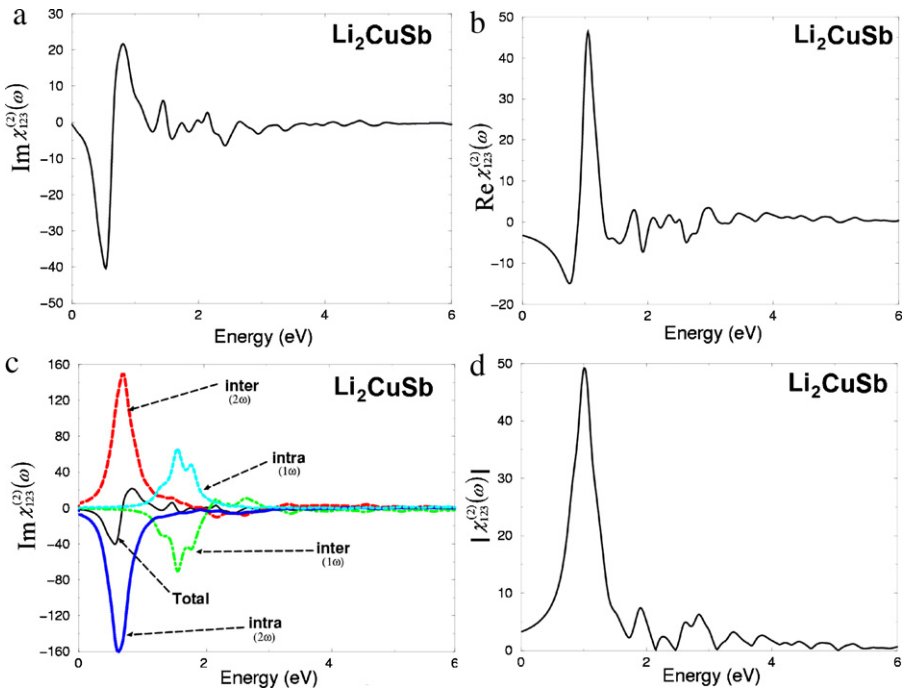

Fig. 6. Calculated complex second-order nonlinear optical susceptibility tensor (a) imaginary part of $\chi^{(2)}_{123}(\omega)$, (b) real part of $\chi^{(2)}_{123}(\omega)$, (c) imaginary part of $\chi^{(2)}_{123}(\omega)$ spectrum along with the intra (2ω)/(1ω) and inter (2ω)/(1ω)-band contributions. (d) the calculated absolute value of $\chi^{(2)}_{123}(\omega)$. The real, imaginary and absolute value of $\chi^{(2)}_{123}(\omega)$ are multiplied by 10^{-7}, in esu units.

The above expressions are written in atomic units with $e^2 = 1/m = 2$ and $\hbar = 1$. Where ω is the photon energy, $P^X_{nn'}(k)$ and $P^Z_{nn'}(k)$ are the X and Z component of the dipolar matrix elements between initial $|nk\rangle$ and final $|n'k\rangle$ states with their eigenvalues $E_n(k)$ and $E_{n'}(k)$, respectively. $\omega_{nn'}(k)$ is the energy difference

$$\omega_{nn'}(k) = E_n(k) - E_{n'}(k) \tag{5}$$

and S_k is a constant energy surface

$$Sk = \{k; \omega_{nn'}(k) = \omega\} \tag{6}$$

When we intercalated Cu_2Sb with Li, it leads to phase transition from tetragonal to cubic structure. The symmetry along the optical axis breaks and measurable amount of second harmonic will generate. The cubic space group F-43m, has only one dielectric tensor component to completely characterize the linear optical properties. This component is $\varepsilon_2(\omega)$ the imaginary part of the frequency dependant dielectric function. The calculation of this frequency dependent dielectric function requires the precise values of energy eigenvalues and electron wavefunctions. These are natural outputs of a band structure calculation. Generally there are two contributions to frequency dependent dielectric functions, namely intra-band and inter-band transitions. The contribution due to intra-band transitions is crucial only for metals. The inter-band transitions of these frequency dependent dielectric functions can be split into direct and indirect transitions. We neglect the indirect inter-band transitions involving scattering of phonons assuming that they give a small contribution to the frequency dependent dielectric functions. To calculate the direct inter-band contributions to the imaginary part of the frequency dependent dielectric function, it is necessary to perform summation over the BZ structure for all possible transitions from the occupied to the unoccupied states. Taking the appropriate transition dipole matrix elements into account, we calculated the imaginary part of the frequency dependent dielectric functions using the expressions in the reference [39]

$$\varepsilon_2(\omega) = \frac{8}{3\pi\omega^2}\sum_{nn'}\int_{BZ}\left|P_{nn'}(k)\right|^2\frac{dS_k}{\nabla\omega_{nn'}(k)} \tag{7}$$

where P $nn'(k)$ is the dipolar matrix elements between initial $|nk\rangle$ and final $|n'k\rangle$ states with their eigenvalues $E_n(k)$ and $E_{n'}(k)$, respectively.

As the investigated compounds are metallic, we must include the Drude term (intra-band transitions) [40].

$$\varepsilon_2(\omega) = \varepsilon_{2\text{inter}}(\omega) + \varepsilon_{2\text{intra}}(\omega) \tag{8}$$

where

$$\varepsilon_{2\text{intra}}(\omega) = \frac{\omega_P\tau}{\omega(1+\omega^2\tau^2)} \tag{9}$$

where ω_P is the anisotropic plasma frequency [41] and τ is the mean free time between collisions.

$$\omega_P^2 = \frac{8\pi}{3}\sum_{kn}\vartheta_{kn}^2\delta(\varepsilon_{kn}) \tag{10}$$

where ε_{kn} is $E_n(k) - E_F$ and ϑ_{kn} is the electron velocity (in basal plane) squared.

Fig. 5a and c depicts the variation of the imaginary part of the frequency dependent dielectric function for the parent and intercalated compounds. The spectral broadening is taken to be 0.1 eV which is typical for the experimental accuracy adopted for dielectric crystals. The effect of the Drude term is significant for energies less than 1 eV. The sharp rise at low energies is due to the Drude term. Following the $\varepsilon_2(\omega)$ spectra one can conclude that $\varepsilon_2^{\perp}(\omega)$ has one main peak located around 2.0 eV, while $\varepsilon_2^{\text{II}}(\omega)$ presented two main peaks situated around 1.5 and 2.0 eV. In the low energy range we noticed there is a considerable anisotropy between the two components $\varepsilon_2^{\perp}(\omega)$ and $\varepsilon_2^{\text{II}}(\omega)$ whereas at energies >4.0 eV both components contribute. After Li's intercalation there is significant

influence on the optical properties resulting in isotropic optical properties and the entire structures shifting towards higher energies with reducing the peaks height.

In general the peaks in the optical response are caused by the allowed electric-dipole transitions between the valence and conduction bands. To identify these structures we should consider the magnitude of the optical dipole matrix elements. The observed structures would correspond to those transitions which have larger optical matrix dipole transition elements. It would be worthwhile to attempt to identify the inter-band transitions that are responsible for the spectral features in $\varepsilon_2(\omega)$ and $\varepsilon_2^{\perp}(\omega)$ and $\varepsilon_2^{\mathrm{II}}(\omega)$ using our calculated band structure and density of states. Following the band structures and density of states we noticed that intercalated Li caused to push the conduction and valence bands towards Fermi energy (E_F) with more bands cuts E_F. This change in the band structures influence the optical transitions and hence the optical properties of the intercalated compound. For simplicity we have labeled the optical transitions in Fig. 2, as A, B and C. The transition A is responsible for the structures in $\varepsilon_2(\omega)$ between 0.0 up to 4.0 eV, B transition is responsible for the structure between 4.0 and 8.0 eV, and C transition is responsible for the structure between 8.0 and 12.0 eV.

The real part of the optical response can be calculated from the spectral dependences of imaginary parts of the dielectric function using Kramers–ronig relations [40], as shown in Fig. 5b and c, again it shows a considerable anisotropy between the parallel and perpendicular components of the optical response for the parent compound.

The spectral features of reflectivity spectra $R(\omega)$ were calculated and illustrated in Fig. 5d and e, for the parent and intercalated compounds. A reflectivity minimum around 2.5 eV and 3.5 eV for the parent and intercalated compound confirms the occurrence of the collective plasma resonance. The depth of the plasma minimum is determined by the imaginary part of the dielectric function at the plasma resonance and is representative of the degree of overlap between the inter-band absorption regions. We notice that a reflectivity maximum around 3.0 and 6.0 eV for the parent and intercalated compound arises from inter-band transitions. We notice that Li's intercalation cause to shift the reflectivity minimum towards higher energies by around 1.5 eV. The parent and the intercalated compounds show high reflectivity at low and high energy ranges. At around 12.5 eV both compounds show rapid increases in the reflectivity. As there are no experimental or theoretical results for the spectral features of the optical susceptibilities available for these compounds, we hope that our work will stimulate more works.

4. Nonlinear response

The parent compound has inversion symmetry and hence SHG is symmetry-forbidden. Intercalated Li within Cu_2Sb results in the loss of inversion symmetry which in turn gives a non-zero SHG. Our aim is to find new materials without inversion symmetry and possess SHG in order to use them as new nonlinear crystals for visible, ultraviolet and infra-red laser radiation at wavelengths that are presently inaccessible via conventional sources. These materials have been in demand for many industrial, medical, biological and entertainment applications. In this work we aim to find novel multi-functional materials which can achieve all the demands for reaching the goal of de-assigning the high technological research tools. The complex second-order nonlinear optical susceptibility tensor $\chi^{(2)}_{ijk}(-2\omega;\omega;\omega)$ has been written elsewhere [42]. It has been demonstrated by Aspnes [43] that only one virtual-electron transitions (transitions between one valence band state and two conduction band states) give a significant contribution to the second-order tensor. Here we ignored the virtual-hole contribution (transitions between two valence band states and one conduction band state) because it was shown to be negative and more than an order of magnitude smaller than the virtual-electron contribution for Li_2CuSb compound. For simplicity we denote $\chi^{(2)}_{ijk}(-2\omega;\omega;\omega)$ by $\chi^{(2)}_{ijk}(\omega)$. The subscripts i, j, and k are Cartesian indices. Insertion of Li into Cu_2Sb leads to phase transition from tetragonal to cubic structure, the symmetry along the optical axis breaks and a measurable amount of second harmonic is generated. For non-centro-symmetric compounds with cubic group symmetry, only one independent nonzero element $\chi^{(2)}_{123}(\omega)$ exists [44,45]. We have calculated the imaginary and real parts of the second-harmonic generation (SHG) susceptibility $\chi^{(2)}_{123}(\omega)$. It is well known that nonlinear optical properties are more sensitive to small changes in the band structure than the linear optical properties. This is attributed to the fact that the second-harmonic response $\chi^{(2)}_{ijk}(\omega)$ involves a 2ω resonance in addition to the normal ω resonance. Both the ω and 2ω resonances can be further separated into inter-band and intra-band contributions.

The imaginary part of the $\chi^{(2)}_{ijk}(\omega)$ optical susceptibility tensor for the lithiated phase Li_2CuSb, is shown in Fig. 6a. We should emphasize that this compound show very high SHG susceptibility. The imaginary part for the SHG susceptibility oscillates around zero in the energy range up to 6.0 eV. We have calculated the complex second-order nonlinear optical susceptibility tensor which contains both the real and the imaginary parts. The real part of $\chi^{(2)}_{ijk}(\omega)$ component is illustrated in Fig. 6b. The inter-band and intra-band contributions to the ω and 2ω resonances are illustrated in Fig. 6c. Following the inter-band and intra-band contributions we note the opposite signs of the two contributions throughout the frequency range and ω resonance is smaller than the 2ω resonance. In the low-energy regime the SHG optical spectra is dominated by the 2ω contributions. In the higher energies the major contribution comes from the ω terms. The structures in Im $\chi^{(2)}_{ijk}(\omega)$ can be understood from the structures in $\varepsilon_2(\omega)$. Unlike the linear optical spectra, the features in the SHG susceptibility are very difficult to identify from the band structure because of the presence of 2ω and ω terms. The first structure in Im $\chi^{(2)}_{ijk}(\omega)$ between 0.0 and 2.0 eV, is associated with interference between a ω resonance and 2ω resonance. The second structure between 2.0 and 4.0 eV is due mainly to 2ω resonance. The last structure from 4.0 to 5.5 is manly due to ω resonance.

In Fig. 6d we show our calculated $\left|\chi^{(2)}_{123}(\omega)\right|$. $\left|\chi^{123}(\omega)\right|$ is calculated from the Im $\chi^{(2)}_{123}(\omega)$ and the Re $\chi^{(2)}_{123}(\omega)$. The structures in $\left|\chi^{(2)}_{123}(\omega)\right|$ can be understood from the structures in $\varepsilon_2(\omega)$ in the same way for the Im. $\chi^{(2)}_{123}(\omega)$. The first peak for this component is located at $2\omega = 1.0$ eV with the peak values of 49.0×10^{-7} esu.

We found that Li_2CuSb possesses high second harmonic generation and its second order optical susceptibility of the total $\left|\chi^{(2)}_{123}(0)\right|$ is equal to 142 pm/V. Based on this value the microscopic second order hyperpolarizability, β_{ijk}, the vector component along the dipole moment direction is about 31.01×10^{-30} esu.

5. Conclusion

In summary, we have made the first-principles electronic structure calculations and predicted that Li_2CuSb should be good electrode materials for high capacity rechargeable batteries and novel materials for second harmonic generation. We hope that these predictions will be checked by further experimental studies. The electronic structure calculation in GGA is carried out by

employing the computer code WIEN2K, which is based on the full-potential linearized augmented-plane-wave method.

Before closing this paper, let us discuss some prospects for future studies of this material, which may include the following: (i) we predict a lithium insertion voltage of 2.78 V for the Li/Cu_2Sb, in good agreement with experimental value (3.0 V). (ii) The volume expansion for the transition from Cu_2Sb to Li_2CuSb is calculated to be 26.5% which is in very good agreement with the experimental data (26.5%) (iii) this material offer an interesting opportunity for studying the effects of intercalation of Li into Cu_2Sb on the electronic properties of parent material. In particular, for using this material as electrodes for high capacity rechargeable batteries and novel materials for second harmonic generation. (iv) the symmetry along the optical axis breaks and a measurable amount of second harmonic generation is generated as a consequence of intercalated Cu_2Sb with Li. (v) we should mention that this compound show very high SHG susceptibility (vi) intercalation of Li leads to phase transfer which may be interested for other studies. (vii) the intercalation leads more bands cuts E_F, resulting in high DOS at E_F and high electronic specific heat coefficient.

Acknowledgements

This work was supported from the institutional research concept of the Institute of Physical Biology, UFB (no. MSM6007665808), the program RDI of the Czech Republic, the project CENAKVA (no. CZ.1.05/2.1.00/01.0024), the grant no. 152/2010/Z of the Grant Agency of the University of South Bohemia. School of Materials Engineering, University Malaysia Perlis (UniMAP) P.O Box 77,d/a Pejabat Pos Besar, 01000 Kangar, Perlis, Malaysia

References

[1] L.M.L. Fransson, J.T. Vaughey, R. Benedek, K. Edstrom, J.O. Thomas, M.M. Thackeray, Electrochem. Commun. 3 (2001) 317.
[2] S. Matsuno, M. Noji, T. Kashiwagi, M. Nakayama, M. Wakihara, J. Phys. Chem. C 111 (2007) 7548–7553.
[3] M.M. Thackeray, J.T. Vaughey, C.S. Johnson, A.J. Kropf, R. Benedek, L.M.L. Fransson, K. Edstrom, J. Power Sources 113 (2003) 124–130.
[4] J. Ren, X. He, W. Pu, C. Jiang, C. Wan, Electrochim. Acta 52 (2006) 1538–1541.
[5] K. Nouneh, I.V. Kityk, R. Viennois, S. Benet, S. Charar, K.J. Plucinski, Mater. Res. Bull. 42 (2007) 236.
[6] J.M. Mosby, A.L. Prieto, J. Am. Chem. Soc. 130 (2008) 10656–10661.
[7] S. Sharma, J.K. Dewhurst, C. Ambrosch-Draxl, Phys. Rev. B 70 (2004) 104110.
[8] M. Morcrette, D. Larcher, J.M. Tarascon, K. Edstrom, J.T. Vaughey, M.M. Thackeray, Electrochim. Acta 52 (2007) 5339–5345.
[9] W. Koch, M.C.A. Holthausen, A Chemistry Guide to Density Functional Theory, Wiley-VCH: Weinheim, New York Chichester, 2000.
[10] R.R. Parr, R.G. Yang, Density Functional Theory of Atoms and Molecules, Oxford University Press, New York, 1989, and references therein.
[11] A.V. Ruban, I.A. Abrikosov, Rep. Prog. Phys. 71 (2008) 046501.
[12] Richard M. More, Klaus Hacker, Phys. Rev. B 2 (1970) 3039.
[13] A.H. Reshak, I.V. Kityk, S. Auluck, J. Chem. Phys. 129 (2008) 074706.
[14] Gao, Shiwu, Comput. Phys. Commun. 153 (190) (2003).
[15] Schwarz, Karlheinz, J. Solid State Chem. 176 (2003) 319.
[16] J.P. Perdew, S. Burke, M. Ernzerhof, Phys. Rev. Lett. 77 (1996) 3865.
[17] P. Hohenberg, W. Kohn, Phys. Rev. B 136 (1964) 864.
[18] P. Blaha, K. Schwarz, G.K.H. Madsen, D. Kvasnicka, J. Luitz, WIEN2K, An Augmented Plane Wave + Local Orbitals Program for Calculating Crystal Properties, Karlheinz Schwarz, Techn. Universitat, Wien, Austria, 2001, ISBN 3-9501031r-r1-2.
[19] O. Jepsen, O.K. Andersen, Solid State Commun. 9 (1971) 1763;
G. Lehmann, M. Taut, Phys. Status Solidi B 54 (1972) 496.
[20] J.A. Wilson, A.D. Yoffe, Adv. Phys. 18 (1969) 193.
[21] S. Sharma, C. Ambrosch-Draxl, Theoretical Investigation of lithiation of intermetallic anode materials: InSb, Cu_2Sb and η'-Cu_6Sn_5, SUPERIONIC CONDUCTOR PHYSICS, Proceedings of the 1st International Discussion Meeting on Superionic Conductor Physics, Kyoto, Japan, 10–14 September 2003, pp. 170–173, 10.1142/9789812706904_0029.
[22] R. Hoffman, Rev. Mod. Phys. 60 (1988) 801.
[23] C.D. Gellatt Jr., A.R. Williams, V.L. Moruzzi, Phys. Rev. B 27 (1983) 2005.
[24] M.E. Arroyo-de Dompablo, J.M. Gallardo-Amores, U. Amador, Electrochem. Solid-State Lett. 8 (2005) 564.
[25] M.E. Arroyo-de Dompablo, U. Amador, F. García-Alvarado, J. Electrochem. Soc. 153 (2006) A673.
[26] F. Zhou, M. Cococcioni, C.A. Marianetti, D. Morgan, G. Ceder, Phys. Rev. B 15 (2004) 235121.
[27] O. Le Bacq, A. Pasteruel, O. Bengone, Phys. Rev. B 69 (2004) 245107.
[28] F. Zhou, C.A. Marianetti, M. Cococcioni, D. Morgan, G. Ceder, Phys. Rev. B 69 (2004) 201101.
[29] M.K. Aydinol, A.F. Kohan, G. Ceder, K. Cho, J. Joannopoulos, Phys. Rev. B 56 (3) (1997) 1354.
[30] A. Van der Ven, M.K. Aydinol, G. Ceder, G. Kresse, J. Hafner, Phys. Rev. B 58 (1998) 2975.
[31] J.S. Braithwaite, C.R.A. Catlow, J.D. Gale, J.H. Harding, P.E. Ngoepe, J. Mater. Chem. 10 (2000) 239.
[32] M.E. Arroyoy de Dompablo, A. Van der Ven, G. Ceder, Phys. Rev. B 66 (6) (2002) 064112.
[33] Y.S. Meng, Y.W. Wu, B.J. Hwang, Y. Li, G. Ceder, J. Electrochem. Soc. 151 (8) (2004) A1134.
[34] M.E. Arroyoy de Dompablo, G. Ceder, J. Power Sources 119 (2003) 654.
[35] Elena Arroyo-de Dompablo M., Ulises Amador, Solid State Sci. 8 (2006) 916–921.
[36] M.M. Thackeray, J. Electrochem. Soc. 142 (1995) 2558.
[37] S. Hufner, R. Claessen, F. Reinert, Th. Straub, V.N. Strocov, P. Steiner, J. Electron Spectrosc. Relat. Phenom. 100 (1999) 191;
R. Ahuja, S. Auluck, B. Johansson, M.A. Kan, Phys. Rev. B 50 (1994) 2128.
[38] A.H. Reshak, C. Xuean, S. Auluck, I.V. Kityk, J. Chem. Phys. 129 (2008) 204111.
[39] M.A. Khan, Arti Kashyap, A.K. Solanki, T. Nautiyal, S. Auluck, Phys. Rev. B 23 (1993) 16974.
[40] Wooten, Optical Properties of Solids, Academic Press, New York and London, 1972.
[41] B. Chakraborrty, W.E. Pickett, P.B. Allen, Phys. Rev. B 14 (1972) 3227.
[42] Ph.D. thesis, Ali Hussain Reshak, Indian Institute of Technology-Rookee, India (2005).
[43] D.E. Aspnes, Phys. Rev. B 6 (1972) 4648.
[44] Huang, Ming-Zhu, W.Y. Ching, Phys. Rev. B 47 (1993) 9449;
Huang, Ming-Zhu, W.Y. Ching, Phys. Rev. B 47 (1993) 9464.
[45] D.J. Moss, J.E. Sipe, H.M. Van Driel, Phys. Rev. B 36 (1987) 9708.